Electrowetting Study of Jumping Droplets on Hydrophobic Surfaces

by

Evelyn Tio

Submitted to the
Department of Mechanical Engineering
in Partial Fulfillment Requirements for the Degree of

Bachelor of Science in Mechanical Engineering

at the

Massachusetts Institute of Technology

June 2014

Signature redacted

Signature of Author: _____
Department of Mechanical Engineering
May 9, 2014

Signature redacted

Certified by: _____
Evelyn N. Wang
Associate Professor of Mechanical Engineering
Thesis Supervisor

Signature redacted

Accepted by: _____
Anette Hosoi
Professor of Mechanical Engineering
Undergraduate Officer

Electrowetting Study of Jumping Droplets on Hydrophobic Surfaces

by

Evelyn Tio

Submitted to the Department of Mechanical Engineering
on May 9, 2014 in Partial Fulfillment of the
Requirements for the Degree of

Bachelor of Science in Mechanical Engineering

ABSTRACT

Recent studies have shown that jumping-droplet-enhanced condensation has higher heat transfer than state-of-the-art dropwise condensing surfaces by ~30-40%. Jumping-droplet condensation occurs due to the conversion of surface energy to kinetic energy during the coalescence of microscale droplets, resulting in droplet ejection from the condenser surface. This conversion of energy is fundamentally studied by using electrowetting to decrease the equilibrium contact angle, increasing droplet surface area. Releasing the voltage allows the droplet to release excess surface energy, causing the droplet to jump off the surface.

In contrast with previous work, droplets were initially held at a static deformed state. Here, jumping from the surface from this static electrowetting-induced state is demonstrated for the first time. Releasing the voltage caused droplets to jump as high as ~2 mm with a maximum conversion efficiency between surface and potential energy of ~5%.

Thesis Supervisor: Evelyn N. Wang

Title: Associate Professor of Mechanical Engineering

Acknowledgements

I would like to express my deepest appreciation to my advisor, Professor Wang, graduate student, Daniel Preston, as well as the rest of the Device Research Laboratory for their invaluable guidance, support and encouragement throughout the year, which made this experience all the more fun and rewarding. I would also like to thank my friends and family for their unwavering support and enthusiasm.

We gratefully acknowledge funding support from the Office of Naval Research (ONR) with Dr. Mark Spector as program manager and the MIT S3TEC Center, an Energy Frontier Research Center funded by the Department of Energy, Office of Science, Basic Energy Science, under Award DE-FG02-09ER46577. This work was performed in part at the Center for Nanoscale Systems (CNS), a member of the National Nanotechnology Infrastructure Network (NNIN), which is supported by the National Science Foundation under NSF award no. ECS-0335765.CNS is part of Harvard University.

Table of Contents

List of Figures

Introduction

Condensation heat transfer is a critical process across a wide spread of industries. Increasing condensation efficiency would allow many of these industries to save energy. For example, condensation heat transfer performance is taken into special consideration when designing heating, ventilation, and air conditioning (HVAC) systems, which account for ~20% of the total energy consumption in developed countries (Li and Yao 2009). HVAC systems are designed to limit condensate buildup and improve energy efficiency. In the power energy industry, condensation heat transfer performance directly influences the thermal efficiency of the steam cycle, which is responsible for over 90% of electrical power generation worldwide (Wiser 2000).

The primary method of condensation is filmwise condensation where a thin film of fluid forms on the surface of the condenser (Nusselt, 1916). Another method is dropwise condensation where drops form on a hydrophobic surface, which is more efficient than filmwise condensation. Any condensate that forms provides a resistance to heat transfer, which increases with condensate thickness. Droplets are small and therefore conduct heat much better than a film of condensate. In both modes, gravity acts as the driving force for removing condensate from the condensing surface. In dropwise condensation, gravity allows droplets to shed from the surface and open new areas for nucleation and droplet growth, resulting in a higher heat transfer coefficient (Schmidt, 1930). However, the force of gravity limits the rate at which drops can shed from the condenser surface.

A recent study has shown that another mode, jumping-droplet condensation, increases heat transfer by 30-40% compared to state-of-the-art dropwise condensation (Miljkovic et al., 2013). Jumping-droplet condensation involves the conversion of surface energy to kinetic energy during coalescence of droplets several orders of magnitude smaller than those shed during dropwise condensation. The excess surface energy from when droplets coalesce on specially designed nanostructured superhydrophobic surfaces causes droplets to jump away from the condensing surface. This jumping-droplet phenomenon can be studied fundamentally through electrowetting, which uses electricity to manipulate the wettability of a droplet.

Figure 1 demonstrates how electrowetting-induced jumping droplets and jumping-droplet condensation share the same fundamental energy conversion process. Figure 1a shows two separate droplets coalescing then subsequently jumping from the surface, while Figure 1b shows an electrowetting-induced droplet jumping as its voltage is released. The two droplets depicted in the first frame of Figure 1a have more cumulative surface energy than the single droplet in the second frame because molecules on the surface of a droplet have more energy than the molecules in the body of the droplet. When the two droplets coalesce, the excess surface energy from the two individual droplets is converted into kinetic energy, which results in ejection of the droplet from the surface. Similarly, the deformed droplet in the first frame of Figure 1b has more surface energy than the original, non-deformed droplet. When the voltage is released, the deformed droplet returns

to its original spherical shape and the excess surface energy is converted into kinetic energy, causing the droplet to jump from the surface.

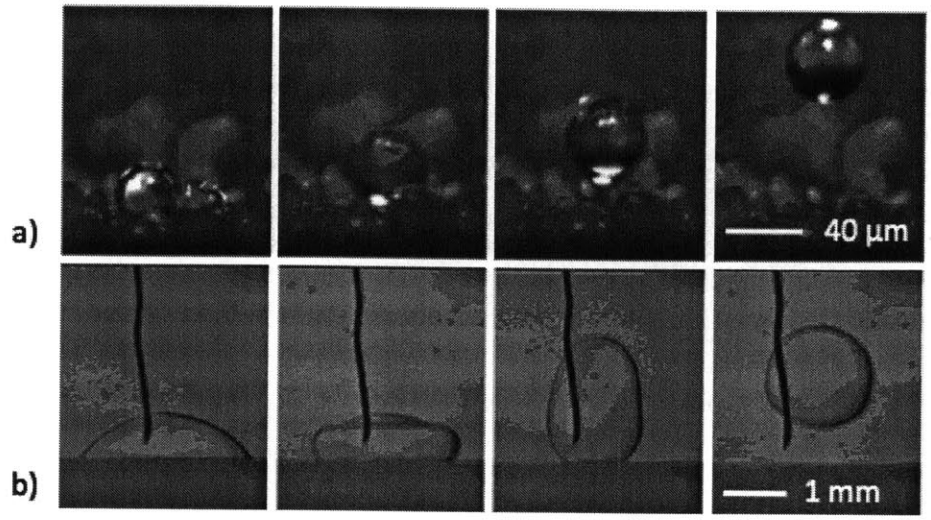

Figure 1. Time-lapse of jumping condensation and EWOD jumping droplet showing how both processes share the same fundamental energy conversion process. **(a)** Two separate droplets coalesce into a single droplet that jumps from the surface. **(b)** A droplet deformed by electrowetting is released and subsequently jumps from the surface.

Using electrowetting to induce droplet jumping will provide insight on the fundamental process of how excess surface energy of a static droplet is converted into the kinetic energy of a jumping droplet.

Background

EWOD History

Electrowetting is a common tool used for handling small-scale droplets. The basis of electrowetting stems from the work of Gabriel Lippmann who in 1875 used electricity to manipulate the wettability of mercury. In 1936, A.N. Frumkin first applied electrowetting to water droplets. Up until the 1990's, applications of

electrowetting were severely limited by electrolytic breakdown caused by using bare electrodes. In 1993, Berge introduced electrowetting-on-dielectric, commonly referred to as EWOD, where an insulator separates the droplet and the conductor. Since then, EWOD has been used in a wide variety of applications including lab-on-chip devices, microfluidics, optical lenses, and electronic displays.

EWOD Theory

The wettability of a droplet sitting on a flat surface is determined by a balance of the surface energies at the three-phase contact line, as shown in Figure 2.

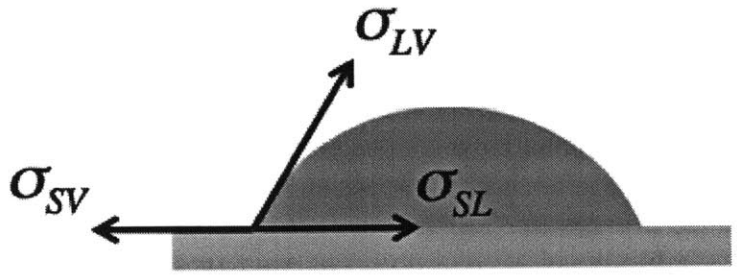

Figure 2. Schematic showing how in equilibrium, the three phases that meet at the line of contact must have a net force per unit length of zero.

The change in energy required to move the contact line where the solid, liquid, and vapor phases meet is:

$$dE = \sigma_{SV} - \sigma_{SL} - \sigma_{LV}\cos(\theta_Y)dx \qquad (1)$$

where σ_{SV}, σ_{SL}, σ_{LV} are the surface energies of the solid/vapor, solid/liquid, and liquid/vapor interfaces, respectively, θ_Y is the equilibrium contact angle, and dx is some differential distance. The equilibrium contact angle can be determined by taking $\frac{dE}{dx} = 0$, which is defined by Young's equation:

$$\cos(\theta_Y) = \frac{\sigma_{SV} - \sigma_{SL}}{\sigma_{LV}} \quad (2)$$

Figure 3 shows a standard EWOD experimental setup.

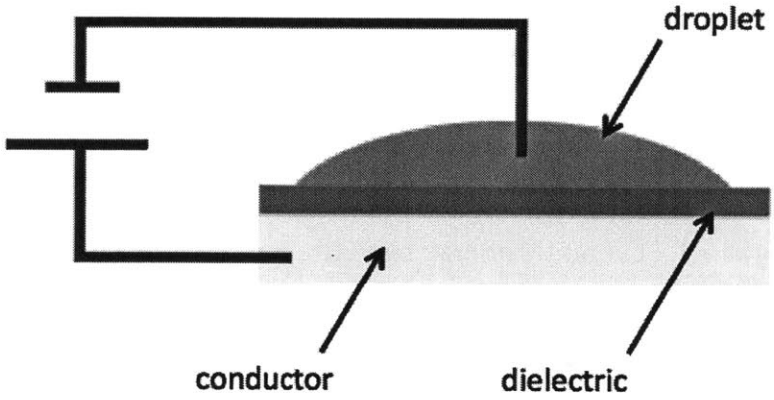

Figure 3. Standard EWOD experimental setup.

A thin dielectric layer of thickness t covers a conductive surface while an electrode is placed into the droplet. When a voltage is applied, the electric double layer at the surface is altered by additional ions lining the dielectric layer and counter-ions lining the solid-liquid interface of the droplet, as shown in Figure 4. This applied voltage results in capacitive storage of energy across the dielectric layer, which can be characterized as a parallel plate capacitor:

$$E_c = \frac{1}{2}\varepsilon_r\varepsilon_0\frac{A}{t}V^2 \quad (3)$$

where ε_r is the relative permittivity, ε_0 is the vacuum permittivity, A is the area of the capacitor plate, t is the separation between plates, and V is the applied voltage.

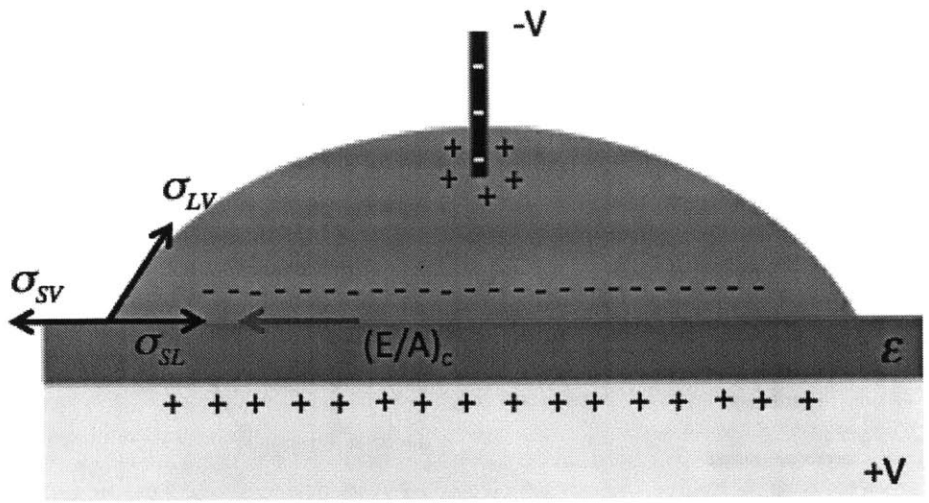

Figure 4. Schematic of electrowetting applied to a droplet.

Rearranging Equation 3 to a per-unit-area basis to match the dimensions of the surface energies in the differential energy balance gives:

$$\cos(\theta_{LY}) = \frac{\sigma_{SV} - \sigma_{SL}}{\sigma_{LV}} + \frac{\varepsilon_r \varepsilon_0 V^2}{2\sigma_{LV} t} \tag{4}$$

which characterizes the Lippmann-Young equilibrium contact angle, θ_{LY}. Substituting in Equation 2 gives θ_{LY} in terms of θ_Y:

$$\cos(\theta_{LY}) = \theta_Y + \frac{\varepsilon_r \varepsilon_0 V^2}{2\sigma_{LV} t} \tag{4}$$

The second term on the right-hand-side of the equation is known as the dimensionless electrowetting number, which is a ratio of the strength of electrostatic energy to surface energy. This quantity is always positive due to the voltage-squared term, meaning that electrowetting always decreases the Lippmann-Young contact angle from the equilibrium contact angle. Theoretically, the observed contact angle should decrease as applied voltage is increased; however, it has been

experimentally shown as voltage is increased, the contact angle saturates to a constant value.

Literature Review

One of the earliest reported instances of jumping droplets is of laser-induced gold nanodroplets (Habenicht et al., 2005). In this study, solid gold triangle nanostructures were melted with laser pulses. The melted gold then immediately contracted to a spherical shape to minimize surface energy, causing gold droplets to jump from the surface. These gold droplets experienced velocities as high as 20 m/s and an energy conversion efficiency from surface energy to kinetic energy of 20%.

In a study focused on characterizing the hydrodynamic flows generated in a droplet when an AC voltage is applied, researchers successfully observed shape oscillations in droplets using AC electrowetting at low frequencies (Ko et al., 2007). These oscillations are a result of the varying electrical force acting on the three-phase contact line. Further studies on oscillating droplets showed oscillation patterns are largely dependent on the applied AC frequency and that oscillating at resonant frequencies maximizes the amplitude of the droplet oscillations (Oh et al., 2008). At large enough frequencies, the center of mass of the droplet moved up and down, sometimes making part of the droplet detach form the surface. This provided evidence that the vibrational energy applied to a droplet through AC electrowetting is significant.

Recent work has used AC electrowetting to demonstrate droplet jumping by bouncing droplets on superhydrophobic and hydrophobic surfaces and show how

this jumping can be used to transport droplets to parallel surfaces suspended above the EWOD surface in three-dimensional microfluidic applications (Lee et al., 2012). By applying sinusoidal electrical signals to 8 μL droplets at 30 Hz, researchers were able to observe droplets jump without fractionation off of a superhydrophobic surface. Jump heights varied with frequency of the signal applied, though the largest height achieved was ~1.5 mm.

Another recent study used electrowetting to gather more insight on the pinning forces involved with capturing and steering drops by determining the critical conditions for capturing sliding drops on an inclined surface (Mannetje et al., 2014). Electrowetting was used to vary the strength of electrical traps along the surface and it was found that the voltage required for trapping a droplet increased as the inclination of the surface increased. It was also found that droplets could be steered along a path by using electrowetting to capture drops and guide them along an existing electrode pattern.

The focus of the current work is to fundamentally study unexplored conditions of EWOD-induced droplet jumping such as water droplets on a hydrophobic surface immersed in silicone oil and jumping from a stationary initial state, as opposed to bouncing the droplet to get it to jump.

Experiment

Setup

The experimental setup, shown in Figure 5, consists of a function generator (AFG3101, Tektronix) passed through a 100x voltage amplifier (A800, FLC electronics) with a positive wire leading to a conductive substrate covered in a dielectric layer and a negative wire leading to a needle electrode that is inserted into the droplet. The experimental stage is back-lit for high-speed video capture (Phantom v7.1, Vision Research) of 100 frames per second. Droplet jumping tests were initially conducted in both air and silicone oil; however, tests conducted in silicone oil proved to be more successful. The silicone oil bath increase the equilibrium contact angle of the droplet, which is relatively low for a water droplet sitting in air. The silicone oil used for experimentation has a viscosity of 0.65 cS, a surface tension in air of 15.9 mN/m, and a density of 760 kg/m^3.

The conductive substrates used for these studies are 1.1 mm thick 25 mm x 25 mm squares of glass covered in a film of ITO that is 120-160 μm thick and has a surface resistivity of 8-12 Ω/sq. The ITO film was then covered with a 4 ±1 μm thick parylene-c layer (VSI Parylene) with a dielectric strength of 22000 V/m and a relative permittivity of $\varepsilon_r \approx 3$. The substrates were connected to the positive lead using steel alligator clips penetrating through the parylene-c coating. The substrate was then placed in a silicone oil bath sitting on a movable stage in front of the high-speed camera. A stainless steel wire with a diameter of 0.125 mm was used as the negative electrode. ImageJ was used to measure important parameters from the

high speed video such as the base radius and height of the deformed droplet and center of gravity of the droplet at the apex of its trajectory.

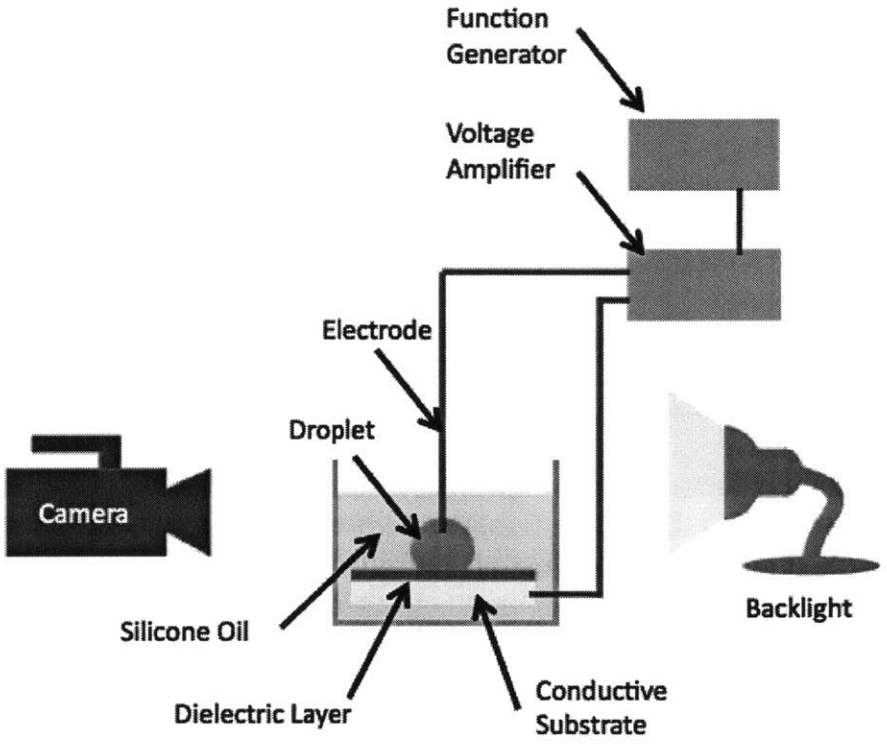

Figure 5. Schematic of experimental setup for water droplets in silicone oil.

Procedure

Droplets of KCl (0.1M in water), which was used to minimize dielectric breakdown, were placed onto the substrate using a syringe and then positioned in front of the camera using the x-y-z controls for the stage. The stainless steel needle was then lowered to impale the droplet. A low applied voltage, starting around 100 V, was initially applied to the droplet. The applied voltage would slowly be increased to a range between 300-400 V, which is where contact angle saturation occurred. High voltages were applied slowly to minimize dielectric breakdown and to obtain the clearest images as possible—applying a voltage to the droplet could

easily move the drop out of focus. The voltage would subsequently be released to observe droplet jumping.

Results

Conversion Efficiency

A time-lapse of a typical instance of a water droplet jumping from an initial resting state is shown in Figure 6.

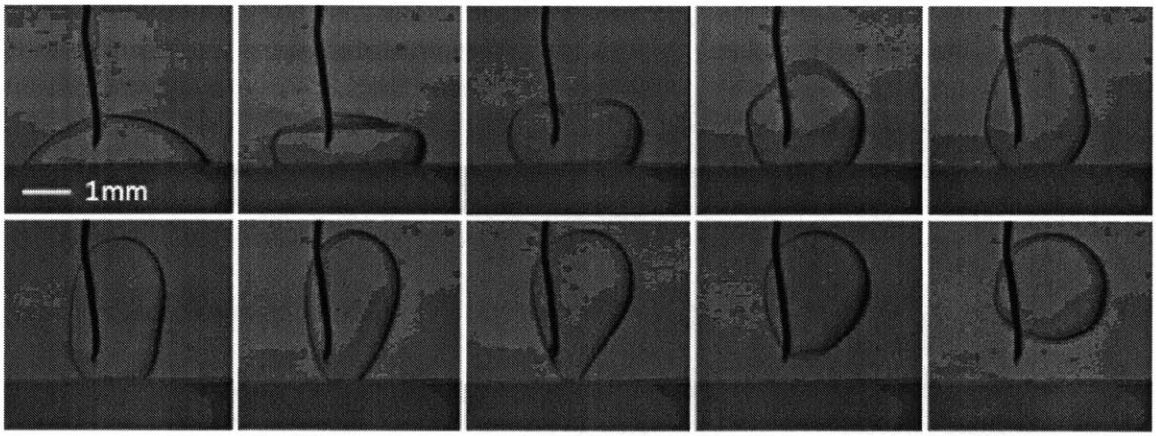

Figure 6. Time-lapse of a water droplet in silicone oil jumping from surface. Electrowetting induces a low contact angle for the droplet. When the voltage is released, the contact angle of the droplet near-instantly changes to restore its original equilibrium contact angle. This causes the droplet to contract towards a spherical shape to minimize energy. As the droplet contracts, surface energy is converted into kinetic energy in the form of flow towards the center of the droplet which then must flow upwards due to the solid boundary beneath the droplet. This upward motion inside the droplet caused by the fluid flow pushes the droplet until it leaves the surface due to its own inertia. Once the droplet reaches its apex where it

has zero velocity and maximum gravitational potential energy, it falls back to the surface. Figure 7 shows a schematic of the progression of energy conversions that occur during this event in an ideal situation where there are no dissipative forces.

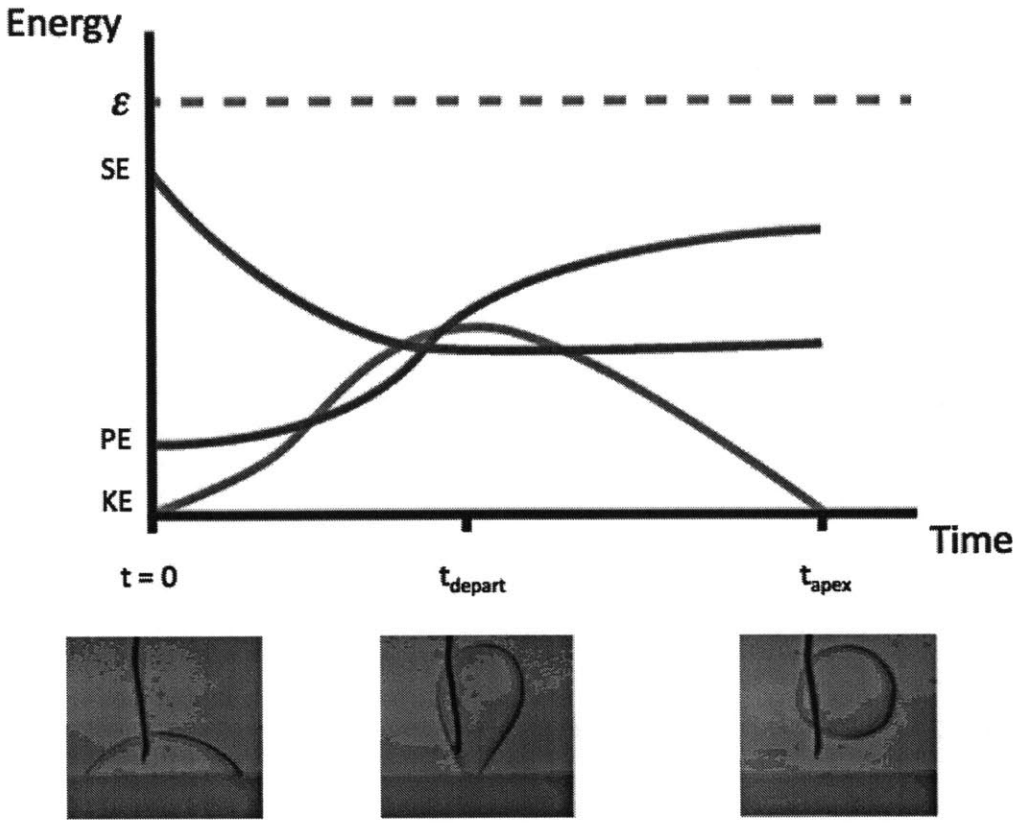

Figure 7. In an ideal case, total energy of the system remains constant as the droplet travels from its deformed state to its apex. Surface energy decreases as the droplet returns to its original shape, potential energy increases as the droplet ascends, and kinetic energy starts at zero, increases, then returns to zero.

In the schematic presented above, ε represents the total energy of the system, SE represents the surface energy, PE represents potential energy, and KE represents kinetic energy. At t =0, the droplet is in its electrowetting-induced deformed state. Surface energy is higher than that of the original spherical shape of the drop, potential energy is low because the deformed droplet's center of mass is close to the surface, and kinetic energy is zero because the droplet is not moving.

After t = 0, the voltage is released and the droplet's contact angle near-instantly reverts back to its equilibrium contact angle, decreasing the droplet's surface area. Once the droplet leaves the surface, it has returned to its original spherical shape, which is why surface energy settles at a constant value after t_{depart}.

Kinetic energy is initially zero at t = 0, but as soon as the voltage is released, the excess surface energy from the deformed droplet is converted into kinetic energy. Kinetic energy slowly increases as fluid flow moves towards the center of the droplet and reaches its maximum value just before t_{depart}. Once the droplet leaves the surface, kinetic energy decreases as the droplet travels towards its apex, where kinetic energy is once again zero.

Potential energy of the system is initially low because the center of mass of the droplet is close to the surface. Once the voltage is released, there is a slow increase in potential energy. Fluid flow is rushing from the edges of the deformed droplet back to the center of the droplet, so the rate of change of the potential energy is very low. As the droplet reverts back to its spherical shape, the rate of change for potential energy increases since the bulk of the droplet is moving in the upwards direction. As the droplet reaches its apex, potential energy plateaus at its maximum value. Because this is a schematic of an ideal situation where energy is conserved, the sum of the surface, kinetic, and potential energy should always be equal to the total energy of the system ε.

In a realistic case, dissipative forces such as viscous drag affect the system, as shown in Figure 8, which depicts the energy profile of a typical experiment. Because energy is not conserved, the maximum potential energy and kinetic energy are

much lower than in the ideal case, resulting in lower jumping height and jumping velocity.

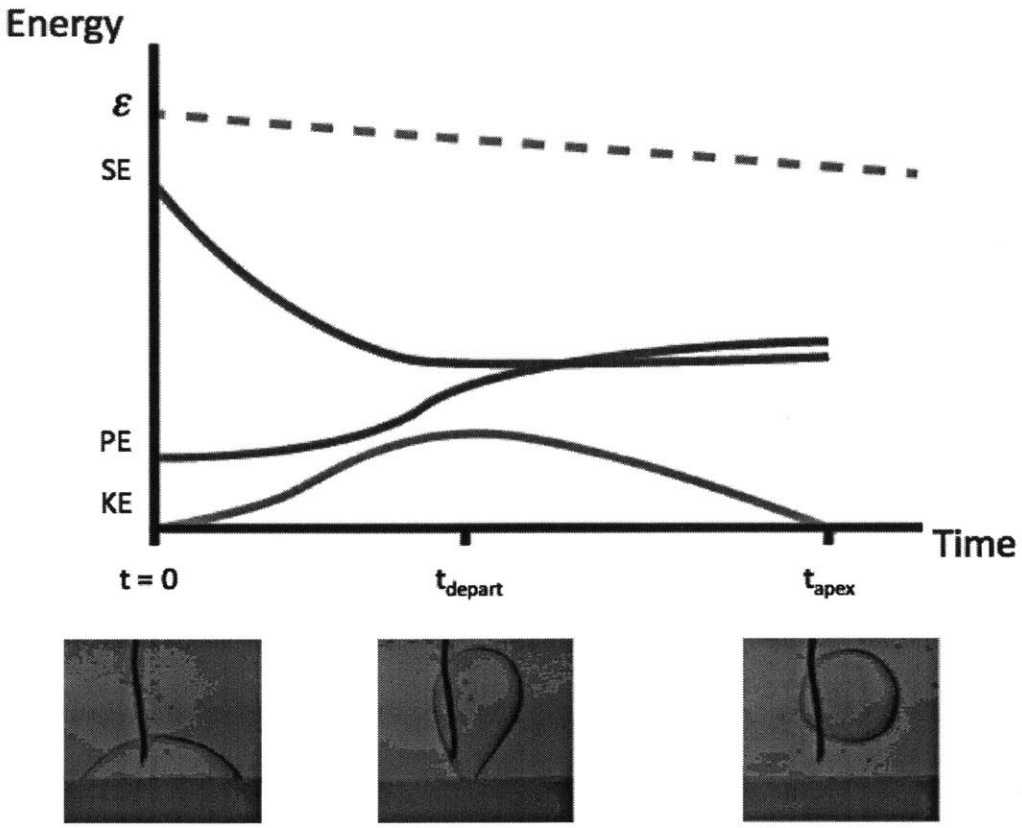

Figure 8. In the experimental case, work done by viscous drag causes total energy of the system to decrease, causing the maximum values of potential energy and kinetic energy to also decrease.

Previous conducting experiments on superhydrophobic surfaces in air reported conversion efficiencies of surface energy to potential energy of 20% studies (Lee et al., 2012); however, the maximum conversion efficiency from this study was $\approx 5\%$. This difference can largely be attributed to the droplets being immersed in silicone oil where viscous drag forces are at play and increase the amount of work needed to detach the droplet and translate the droplet to its maximum height. Another reason for the discrepancy could be that the experiments

done by Lee were conducted using a sine wave with low frequency to apply a voltage to the droplet, inducing an oscillating motion before the droplet leaves the surface and resulting in a buildup of energy over time. For this study, either a sine wave with a frequency of 10 kHz or a constant DC voltage was used to induce the EWOD-jumping from an initial resting state.

Droplet sizes ranged from 3 μL to as large as 12 μL and jumped as high as ~ 2 mm. Results showed that conversion efficiency between surface energy and potential energy increased as droplet size increased, as depicted in Figure 9.

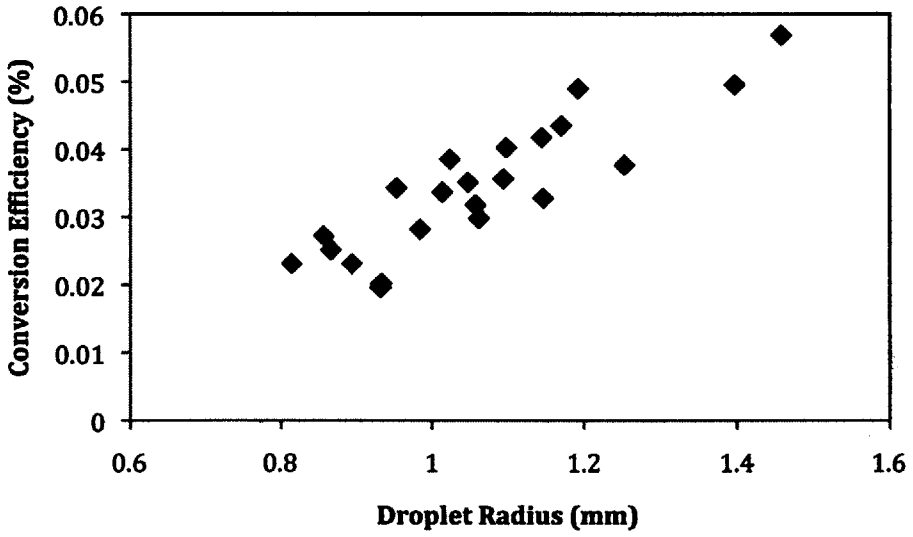

Figure 9. Experimental results show that conversion efficiency increases as droplet radius increases.

This trend is due to the viscous drag effects from the silicone oil the experiments were conducted in. The Reynolds number for these jumping droplets is greater than 1, so the viscous drag effects observed are a result of form drag. The surface energy of a droplet scales with R^2 while the work done by form drag of a droplet scales with just R. This means that on a smaller scale, work done by viscous drag has a much

larger effect on the overall conversion efficiency, but as droplet size increases, losses from drag are not as significant compared to the overall surface energy of the droplet.

This relationship between radius and conversion efficiency can be verified by considering losses from drag in the energy balance. Assuming initial kinetic energy is approximately initial surface energy, we can solve for the initial velocity. Using this initial velocity in the form drag equation, we can approximate the work dissipated by drag. By defining conversion efficiency as the surface energy minus work due to drag divided by surface energy, the relationship between droplet radius and conversion efficiency is shown to scale as:

$$\varepsilon_{conv} = 1 - \frac{1}{\frac{\rho g}{\gamma} R^2 + 1} \tag{5}$$

The complete derivation can be found in the supplementary notes. Overlaying Figure 9 with this characteristic equation shows that this scaling argument agrees with the experimental data, as shown in Figure 10. The theoretical curve sits slightly above the experimental data because average velocity was used to calculate the jumping droplet's Reynolds number. Initial velocity, which is typically larger than average velocity, was used in the scaling argument, meaning the theoretical curve slightly overestimates conversion efficiency. Figure 10 validates the trend determined from the scaling argument provided in Equation 5, which shows that the drag force on the droplet as it travels through silicone oil is responsible for the low conversion efficiencies.

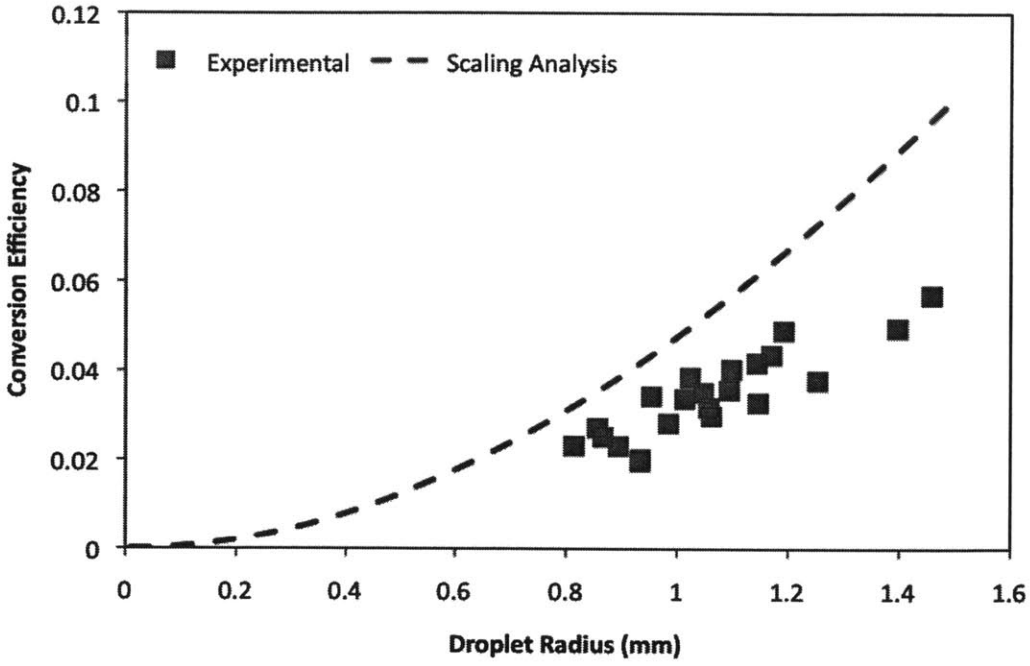

Figure 10. Overlaying experimental data with the characteristic equation derived from the scaling argument shows that the resulting equation agrees with the data collected.

Droplet Pinch-off

When a large voltage is initially applied to the droplet as a Heaviside step function, as opposed to steadily ramping the voltage and keeping the droplet in a quasi-static state, sometimes the droplet would split into two as the contact angle transitioned from a high to low. This pinch-off can be seen in Figure 12.

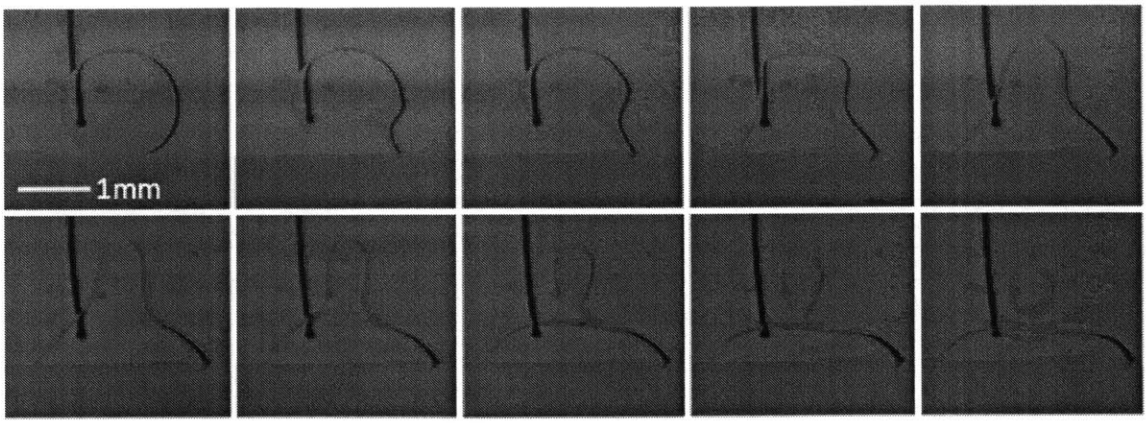

Figure 11. Time-lapse of the droplet pinching off when 360 V at 10 kHz is applied to a resting droplet.

The pinch-off occurs due to the droplet's resting inertia in combination with the large voltage applied to the droplet, which results in a drastic decrease in the contact angle. This decreased contact angle draws fluid away from the centerline of the droplet. In the instance shown in Figure 12, the kinetic energy of the fluid flow is high enough to overcome the interfacial energies holding the droplet together, causing the top part of the droplet to pinch off from the main droplet. From a force perspective, the interfacial tension around the pinch-off site was not great enough to accelerate the pinched-off droplet section downwards at the same rate as the main droplet. Droplet splitting was only observed for high voltages (> 300 V). At lower voltages, such as 200 V, the droplet exhibited similar behavior with fluid flow rushing outwards and pulling the top of the droplet down, but the pull from the fluid flow was not strong enough to overcome the surface tension of the droplet and cause it to pinch-off.

Conclusion

Past studies have utilized droplet vibration at resonant frequencies to build up enough energy to make droplets jump from a surface. The present work demonstrates experimentally for the first time droplets jumping from an initial static deformed state induced by electrowetting. Although jumping heights achieved with EWOD-induced droplet jumping were comparable to jumping heights achieved via droplet vibration-induced jumping, the conversion efficiency between surface energy and potential energy was found to be much lower (~ 5%) than other studies that have reported conversion efficiencies of ~20%. The difference in these efficiencies can largely be attributed to the fact that the experiments for this study were conducted in a bath of silicone oil to reduce contact angle hysteresis of water. Conducting these experiments in oil introduced losses due to drag and decreased the conversion efficiency accordingly, as shown through scaling arguments. This study has also demonstrated EWOD-induced droplet pinch-off, which might be useful for transport or controlling droplet size in microfluidic applications.

Up until this point, studies regarding EWOD have mainly centered on using droplet oscillations to eject droplets from a surface. However, the results from this study have shown that resonant electrical actuation is not the only way to achieve droplet jumping. The increased surface area of a static deformed droplet provides enough energy to cause a droplet to jump from the surface. The parylene-c coating on the surfaces used in this study not only served as a dielectric layer, but also as a hydrophobic coating. In air, the water droplet's relatively low equilibrium contact angle was not conducive to droplet jumping, so experiments were conducted with

the samples submerged in a bath of silicone oil to increase equilibrium contact angle and also reduce contact angle hysteresis. Future studies should investigate how EWOD-induced jumping droplets from an initial static deformed state behave in air, using superhydrophobic surfaces to achieve high contact angles for droplets and minimize adhesion to the surface. Many current applications of electrowetting revolve around translating drops in the two-dimensional plane, but EWOD-induced jumping droplets would allow control of droplet movement in a third dimension which has application in digital microfluidics. Having three-dimensional control over a droplet would simplify the complicated fabrication process for 3D microfluidic channels.

Previous studies regarding jumping droplet condensation found that coalescence occurred best when droplet radii were small between a range of 10-100 μm (Boreyko & Chen, 2009). However, the experimental results from the current study have shown that a larger droplet radius is favorable when jumping droplets are induced in a fluid medium. This information may be useful in understanding jumping droplets behavior in the presence of non-condensible gases, which increase the surrounding fluid's density and viscosity as compared to experiments performed with pure water vapor. Finally, this work provides a surface-to-kinetic energy conversion for droplets initially at rest analogous to that observed for droplets jumping during condensation on superhydrophobic surfaces, which offers insight into the fundamental jumping droplet mechanism.

Bibliography

Boreyko, J.B., Chen, C.H., (2009). Self-propelled dropwise condensate on superhydrophobic surfaces. *Phys Rev Lett, 103*, p. 184501-184504.

Habenicht, A., Olapinski, M., Burmeister, F., Leiderer, P., & Boneberg, J., (2005). Jumping Nanodroplets. *Science, 309*, p. 2043.

Ko, S. H., Lee, H. & Kang, K. H., (2008). Hydrodynamic Flows in Electrowetting. *Langmuir, 24* p. 1094-1101.

Lee, S. J., Lee, S., & Kang, K. H., (2011). Jumping of a droplet on a superhydrophobic surface in AC electrowetting. *J Vis, 14*, p. 259-264.

Li, B., Yao, R., (2009). Urbanisation and its impact on building energy consumption and efficiency in China. *Renewable Energy, 34*, p.1994-98.

Mannetje, D., Ghosh, S., Lagraauw, R., Otten, S., Pit, A., Berendsen, C., Zeegers, J., Ende, D., & Mugele, F., (2014). Trapping of drops by wetting defects. *Nature Communications, 5*, doi:10.1038/ncomms4559.

Miljkovic, N., Enright, R., Youngsuk, Nam., Lopez, K., Dou, N., Sack, J., Wang, E. N., (2013). Jumping-Droplet-Enhanced Condensation on Scalable Superhydrophobic Nanostructured Surfaces. *Nano Letters 13(1)*, p. 179-187.

Nusselt, W., (1916). Die Oberflächenkondesation des Wasserdampfes, Z. Ver. Dt. Ing., 60(27), p. 541-46.

Oh, J. M., Ko, S. H., & Kang, K. H., (2008). Shape Oscillation of a Drop in ac Electrowetting. *Langmuir, 24*, p. 8379-8386.

Schmidt, E., Schurig, W., & Sellschopp, W., (1930). *Tech. Mech. Thermodyn, 1*, 53-63.

Wiser, R., Bolinger, M., & Holt, E., (2000). Customer Choice and Green Power in the United States: How Far Can It Take Us? *Energy and Environment, 11(4)*, p. 461-477

Appendix A: Data Extraction

ImageJ was used to extract important parameters from captured high-speed video as shown below.

The deformed droplet base diameter and height were needed to calculate surface area and volume of the initial droplet:

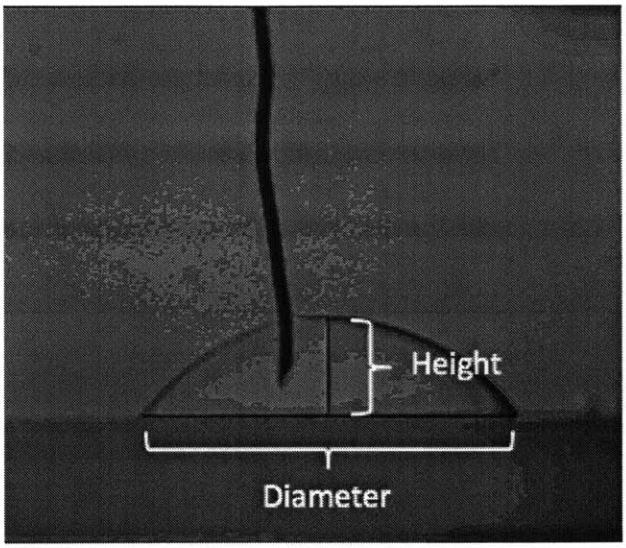

Figure 12. The height and base radius of the deformed droplet were measured using ImageJ.

The center of gravity height of droplet at the apex of its jump was needed to calculate maximum potential energy:

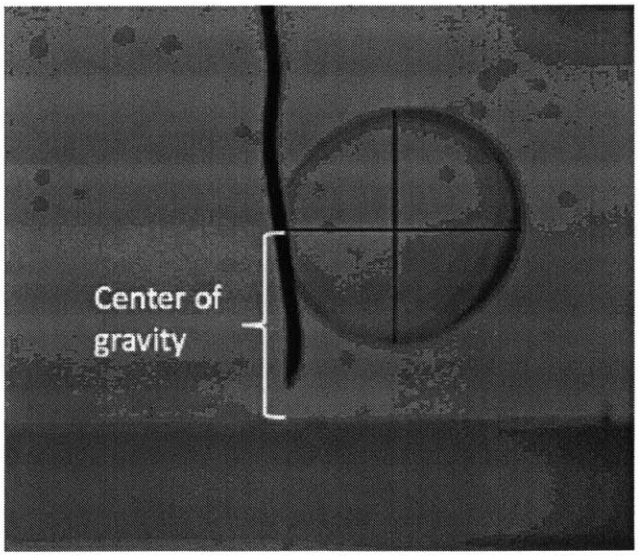

Figure 13. The center of gravity of the droplet at the apex of its jump was measured using ImageJ.

Appendix B: Data Processing

The following MATLAB code was used to calculate experimental values based on parameters extracted from the high-speed video.

```
clear
clc
% Calculating energy efficiency of droplet jumping process

% Define all variables

%Properties of Deformed Droplet
a =1841.779975e-6 ; % base radius in m
h_cap = 874.9227441e-6 ; % height of cap in m

%Propeties of Spherical Droplet
CoG_sphere = 1535.460445e-6; % center of gravity for sphere in m

%Other Constants
g = 9.81; % gravity in m/s^2
gamma_w_p = 0.0505; %water surface tension polar comp (N/m)
gamma_w_d = 0.0223; %water surface tension dispersion comp (N/m)
gamma_o_d = 0.0159; %oil surface tension dispersion (N/m)
gamma_p_d = 0.020; %parylene-c surface tension (N/m)
p_w = 997; %density of water (kg/m^3)
p_o = 760; %density of silicone oil (kg/m^3)

% Surface Area Calculations

SA_sphere = 4*pi*r_sphere^2; %calculated surface area of sphere
r_cap = (a^2+h_cap^2)/(2*h_cap); %calculated radius of deformed droplet
SA_cap = 2*pi*r_cap*h_cap; %calculated surface area of deformed droplet
A_cap = pi*a^2;%calculated area of droplet base
SA_deformed = SA_cap + A_cap;
V_droplet = 4/3*pi*r_sphere^3;
V_cap = (pi*h_cap/6)*(3*a^2+h_cap^2); %calculated volume of droplet
r_sphere_calc = (3*V_cap/(4*pi))^(1/3);
SA_sphere_calc = 4*pi*r_sphere_calc^2;
V_sphere_calc= (4/3)*pi*r_sphere_calc^3;

dSA = SA_deformed - SA_sphere; %difference in surface areas


% Surface Energy Calculations

gamma_wo = gamma_w_p + gamma_w_d + gamma_o_d -
2*sqrt(gamma_w_d*gamma_o_d); %water-oil surface tension

gamma_wp = gamma_w_p + gamma_w_d + gamma_p_d -
2*sqrt(gamma_w_d*gamma_p_d); %water-parylene surface tension

SE_deformed = gamma_wo*SA_cap + gamma_wp*A_cap;
```

```
SE_sphere = gamma_wo*SA_sphere_calc; %using calculated radius from
initial V

dSE = SE_deformed-SE_sphere;

%Potential Energy Calculations

CoG_cap_center = (3*(2*r_cap-h_cap)^2)/(4*(3*r_cap-h_cap)); %distance
above center of the sphere

CoG_cap = h_cap - r_cap + CoG_cap_center;

h_expected = (dSE/((p_w-p_o)*V_cap*g))+ CoG_cap; %calculated expected
height from initial change in surface energy

PE_initial = (p_w-p_o )*V_cap*g*CoG_cap;

PE_final = (p_w-p_o)*g*V_cap*CoG_sphere;

dPE = PE_final - PE_initial;


%Energy Efficiency

conversion_efficiency = (dPE/dSE);

results = [V_cap;SA_cap; SA_deformed; SA_sphere; SE_deformed;
SE_sphere; dSE; CoG_cap;
CoG_sphere;h_expected;PE_initial;PE_final;dPE;total_efficiency;conversi
on_efficiency]
```

Appendix C: Scaling Derivation

The following is a derivation for the scaling argument showing that by taking into account the losses from drag, conversion efficiency should increase as radius increases.

Surface energy scales with:

$$SE \sim \gamma R^2 \tag{C1}$$

where γ is surface tension and R is the droplet radius.

Kinetic energy scales with:

$$KE \sim mv^2 \sim \rho R^3 v^2 \tag{C2}$$

where $\rho = \Delta\rho$ to account for the different densities of water and silicone oil.

If we assume that kinetic energy is approximately equal to the initial surface energy:

$$KE \sim SE \sim \rho R^3 v^2 \sim \gamma R^2 \tag{C3}$$

Now solve for initial velocity v:

$$v \sim \sqrt{\frac{\gamma}{\rho R}} \tag{C4}$$

The work dissipated by form drag is:

$$W_d \sim \rho h v^2 R^2 \tag{C5}$$

Where h is the maximum height of the droplet.

Using the initial velocity defined in Equation C4 as an approximate velocity, which over-approximates the work done by drag:

$$W_d \sim h\gamma R \tag{C6}$$

Conversion efficiency is defined as:

$$\varepsilon = \frac{SE - W_d}{SE} \sim \frac{\gamma R^2 - h\gamma R}{\gamma R^2} \tag{C7}$$

h in Equation C7 can be approximated by assuming that the difference between surface energy work done by drag is equal to final potential energy:

$$SE - W_d = PE \approx \rho R^3 gh \tag{C8}$$

$$\rho R^3 gh \approx \gamma R^2 - h\gamma R \tag{C9}$$

Solving for h:

$$h \approx \frac{\gamma R}{\rho g R^2 + \gamma} \tag{C10}$$

Using this h for conversion efficiency defined in Equation C7 and rearranging:

$$\varepsilon_{conv} \approx 1 - \frac{1}{\frac{\rho g R^2}{\gamma} + 1} \tag{C11}$$

The term $\frac{\rho g}{\gamma}$ is a constant dependent on material properties with units of $m^{1/2}$, leaving the approximation:

$$\varepsilon_{conv} \approx 1 - \frac{1}{R^2 + 1}$$